The fatty liver dystrophy mutant mouse: microvesicular steatosis associated with altered expression levels of peroxisome proliferator-regulated proteins

Stefan Rehnmark,[1,*] Carol S. Giometti,[†] Bernard G. Slavin,[§] Mark H. Doolittle,[*] and Karen Reue[2,*]

Lipid Research Laboratory,* West Los Angeles VA Medical Center and Department of Medicine, University of California, Los Angeles, CA 90073; Protein Mapping Group,[†] Argonne National Laboratory, Argonne, IL 60439; and Department of Cell and Neurobiology,[§] University of Southern California, Los Angeles, CA 90033

Abstract **Fatty liver dystrophy (*fld*) is an autosomal recessive mutation in mice characterized by hypertriglyceridemia and fatty liver during neonatal development. The fatty liver in *fld/fld* mice spontaneously resolves between the age of 14–18 days, at which point the animals develop a neuropathy associated with abnormal myelin formation in peripheral nerve. We have investigated the morphological and biochemical alterations that occur in the fatty liver of neonatal *fld/fld* mice. Studies at the light and electron microscopic level demonstrated the accumulation of lipid droplets and hypertrophic parenchymal cells in *fld* neonates, with no apparent liver pathology after resolution of the fatty liver. To better characterize the biochemical basis for the development of fatty liver in *fld* mice, we compared protein expression patterns in the fatty liver of *fld* mice and in the liver of phenotypically normal (wild-type) littermates using quantitative two-dimensional gel electrophoresis. We detected 24 proteins with significantly altered expression levels ($P < 0.001$) in the *fld* fatty liver, 15 of which are proteins that are altered in abundance by peroxisome proliferating chemicals. As these compounds characteristically elicit changes in the expression of mitochondrial and peroxisomal enzymes involved in fatty acid oxidation, we quantitated rates of fatty acid oxidation in hepatocytes isolated from *fld* and wild-type mice. These studies revealed that hepatic fatty acid oxidation in *fld* neonates is reduced by 60% compared to wild-type littermates. In hepatocytes from adult *fld* mice that no longer exhibit a fatty liver, oxidation rates were similar to those in hepatocytes from age-matched wild-type mice. These findings indicate that altered expression of proteins involved in fatty acid oxidation is associated with triglyceride accumulation in the *fld* fatty liver.**—Rehnmark, S., C. S. Giometti, B. G. Slavin, M. H. Doolittle, and K. Reue. **The fatty liver dystrophy mutant mouse: microvesicular steatosis associated with altered expression levels of peroxisome proliferator-regulated proteins. *J. Lipid Res.* 1998.** 39: **2209–2217.**

Supplementary key words triglyceride • 2-dimensional gel electrophoresis • hepatocytes

Fatty liver (hepatic steatosis) occurs in association with a wide range of diseases, toxins, and drugs (reviewed in ref. 1). The majority of clinically significant occurrences are related to excessive alcohol intake, diabetes, obesity, and cachexia resulting from debilitating disease. Less prevalent causes of fatty liver include inborn errors in fatty acid β-oxidation or urea cycle enzymes, Reye's syndrome, acute fatty liver of pregnancy, protein–calorie malnutrition, and drug toxicity. Some evidence suggests that an individual's susceptibility to developing fatty liver may be determined, in part, by genetic factors (2). Although some forms of fatty liver have traditionally been considered clinically benign, it is now clear that steatosis can lead to the development of more advanced liver pathology. It therefore becomes important to elucidate the genes and underlying biochemical mechanisms that contribute to the development and progression of fatty liver.

As only limited aspects of the development of hepatic steatosis can be investigated directly in humans, experimental animal models fulfill an important role in studies aimed at defining the underlying biochemical derangements. In this study, we further characterize the fatty liver in a mutant mouse strain known as fatty liver dystrophy (*fld*). *Fld* is a recessive mutation that spontaneously arose in the BALB/cByJ mouse strain in 1981 (3). Thus, only mice homozygous for mutant alleles at the *fld* locus (*fld/fld* genotype) exhibit the fatty liver phenotype; heterozygotes (+/*fld* genotype) appear phenotypically normal, and cannot be distinguished from mice homozygous for the wild-type allele (+/+ genotype)[3]. The *fld* animals ap-

Abbreviations: *fld*, fatty liver dystrophy; apo, apolipoprotein; 2DE, two-dimensional gel electrophoresis.

[1]Current address: Department of Metabolic Research, Stockholm University, Stockholm, Sweden.

[2]To whom correspondence should be addressed.

[3]Throughout the text, the term "*fld*" is used to indicate mice of the *fld/fld* genotype, and "wild-type" is used to indicate mice of genotypes +/+ and +/*fld*, both of which appear phenotypically normal.

pear normal at birth, but upon suckling, rapidly develop an enlarged fatty liver that is evident by the distended appearance of the abdomen and blanched white liver, which can be seen through the skin of the neonatal mice. The excess lipid in the liver is virtually all triglyceride, with a slight elevation in diglycerides, but no apparent changes in cholesterol, cholesteryl ester, or phospholipids (4). Concomitant with the appearance of the fatty liver, neonatal *fld* mice exhibit hypertriglyceridemia (1000 mg/dL), elevated hepatic mRNA levels for apolipoproteins (apo) A-IV and C-II, and diminished hepatic lipase mRNA levels and activity (3). In addition, lipoprotein lipase activity is greatly diminished in white adipose tissue, although activity is normal or only slightly reduced in liver, brown adipose, and heart.

Notably, triglyceride levels in liver and blood of *fld* mice spontaneously return to normal at the suckling/weaning transition at postnatal days 13–18 (3). Although this reversion coincides with the change from a diet that is rich in triglycerides (mother's milk) to one that is low in fat and high in carbohydrates (mouse chow), two lines of evidence indicate that the resolution is a genetically programmed event, and not the result of a change in diet. *1*) In *fld* mice fed mother's milk for a prolonged period without weaning, the fatty liver returns to normal on the same schedule as in weaned mice; and *2*) after weaning, feeding *fld* mice a triglyceride-rich diet fails to elicit a fatty liver or hypertriglyceridemia (3).

After resolution of the fatty liver, the primary outward manifestation of the *fld* mutation is a neuropathy characterized by an unsteady gait and loss of control of the hind legs. This neuropathy has been attributed to abnormalities in formation and maintenance of the myelin sheath in the peripheral nerve (5). The *fld* mutation has been mapped to a single locus on mouse chromosome 12 (6), indicating that the lipid and nerve abnormalities in *fld* mice most likely result from a mutation occurring within a single gene. Thus, the *fld* mutation represents a model for elucidating mechanisms that contribute to both the development and resolution of steatosis and subsequent manifestation of peripheral neuropathies associated with dyslipidemias.

We have investigated the morphological and biochemical alterations that occur in the fatty liver of neonatal *fld* mice. Light and electron microscopic studies reveal microvesicular steatosis in hepatocytes of neonatal *fld* mice, with no apparent pathology in the liver of adult *fld* mice. To better characterize the biochemical basis for the development of fatty liver in *fld* mice, we compared protein expression patterns in the fatty liver of *fld* mice and in the liver of wild-type littermates using quantitative two-dimensional gel electrophoresis. The *fld* fatty liver exhibited elevated expression levels of several proteins known to be altered in abundance by peroxisome proliferating compounds. As these compounds regulate the expression of enzymes involved in fatty acid oxidation, we quantitated rates of fatty acid oxidation in hepatocytes isolated from *fld* and wild-type mice. Our findings indicate that altered expression of proteins involved in fatty acid oxidation is associated with triglyceride accumulation in the *fld* fatty liver.

METHODS

Animals

Non-tested breeding pairs of mouse strain BALB/cByJ-*fld* were obtained from the Mouse Mutant Resource colony at the Jackson Laboratory (Bar Harbor, ME). All mice were maintained in a 12-h light/dark cycle and fed Purina Mouse Chow 5001 ad libitum. Pairs were bred continually for up to 6 months to produce *fld*/*fld* and wild-type (+/?) offspring used in these studies. All animals received humane care as outlined in the "Guide for the Care and Use of Laboratory Animals."

Light and electron microscopy

Mice were anesthetized with isoflurane (Forane, Ohmeda PPD, Inc.) and livers were fixed by whole body intracardiac perfusion of a solution consisting of 2% paraformaldehyde and 2% glutaraldehyde in 0.1 M cacodylate buffer. Portions of the right lobes of liver were excised, diced into 1–2 mm blocks, and placed into the above fixative for 30 min. This was followed by postfixation of the blocks with 1% osmium tetroxide for 1 h. Tissue blocks were rinsed in cacodylate buffer, dehydrated in ethanol, and embedded in Polybed 812 epoxy resin. Semi-thin sections were deplasticized in alcoholic sodium hydroxide, stained with toluidine blue, and photographed with an Olympus AH-2 light microscope. Thin sections for electron microscopic analysis were stained with lead and uranium salts and examined in a JEOL 1200X electron microscope.

Hepatic triglyceride measurements

Lipid extracts were prepared from the livers of 6-day-old wild-type and *fld* mice and triglycerides were determined enzymatically (Triglycerides-GB Reagent Kit, Boehringer Mannheim Diagnostics, Indianapolis, IN) as described (7).

Quantitative 2-dimensional gel electrophoresis (2DE)

Livers were harvested from 5–7-day-old *fld*/*fld* and wild-type mice and immediately frozen in liquid nitrogen until processing. In preparation for electrophoresis, livers were homogenized in 1 ml of a solution containing 9 M urea, 4% Nonidet P-40, 5% β-mercaptoethanol, and 2% pH 9–11 ampholytes per 250 mg (frozen tissue weight) (8). The homogenate was centrifuged for 5 min at 100,000 rpm (435,000 *g*) in a Beckman TL 100 ultracentrifuge, and the supernatant was decanted.

2DE was carried out with 10 individual livers of each phenotype (i.e., 10 *fld*/*fld* and 10 wild-type). For electrophoresis in the first dimension, 10 μl of liver homogenate (0.25 mg protein) was loaded onto polyacrylamide rods containing an equal mixture of Biolyte pH 3–10 and pH 5–7 ampholytes. Second dimension electrophoresis was performed on 10–17% SDS polyacrylamide gradient gels. Gels were fixed, stained in 0.125% Serva blue R (Coomassie blue R250)/2.5% (vol/vol) H_3PO_4/50% ethanol), and destained in 20% ethanol. 2DE patterns were digitized using an Eikonix 1412 scanner and spot matches were made by an automatic matching algorithm. Spot densities were integrated to detect proteins showing statistically significant differences between *fld*/*fld* and wild-type samples ($P < 0.001$).

Primary hepatocyte isolation

Hepatocytes were isolated by recirculating perfusion of livers from 12-day-old and adult mice as described (9). Perfusion of the

livers from young mice was made possible by the use of extra fine tubing (0.5 mm diameter) for cannulation of the portal vein (Bio-Time, Inc., Berkeley, CA). Primary hepatocytes were cultured in arginine-free Dulbecco's modified Eagle's medium (Life Sciences, Grand Island, NY) containing 10% fetal calf serum at 37°C in 5% CO_2. The use of arginine-free medium prevents the growth of fibroblasts that may be present in hepatocyte preparations from neonatal mice.

Hepatic lipase activity assay

Hepatic lipase activity in hepatocyte culture medium was determined using a tri[^{3}H]oleate substrate (10). Three culture plates each for wild-type and *fld* hepatocytes were treated with heparin (10 U/ml) for 24 h, and 50-μl aliquots were removed for assays performed in duplicate from each plate. In measurements presented, one mU of enzyme activity represents the release of 1 nmol of fatty acid per min.

Northern blot analysis

Total RNA was isolated from cultured hepatocytes by extraction with TriZol (Gibco BRL, Gaithersburg, MD). RNA (10 μg) was electrophoresed in formaldehyde gels, blotted, and hybridized to ^{32}P-labeled cDNA probes for mouse apoA-IV and apoA-I as described (11).

Palmitate oxidation assay

Freshly isolated hepatocytes were plated at a density of 10^5 cells/well in 24-well tissue culture plates (one well = 2 cm^2). Plates were incubated 20 h at 37°C in 5% CO_2. Palmitate oxidation was assayed using a [9,10(n)^{3}H]palmitate substrate (54 Ci/mmol, Amersham, Arlington Heights, IL) by the method of Moon and Rhead (12). Briefly, cell monolayers were rinsed twice with phosphate-buffered saline and incubated in 0.2 ml of substrate mixture containing 22 μm unlabeled palmitate + 5 μCi [^{3}H]palmitate in Hank's basic salt solution (Life Sciences, Grand Island, NY) containing 0.5 mg/ml BSA. Negative controls were prepared by treating the monolayer with methanol for 30 s to abolish cellular metabolism. In initial studies, cells were incubated in the palmitate reaction mixture for times ranging from 15 min to 3 h to ascertain linearity of the assay. For data presented, 2 h was used, at which time the reaction medium was collected from the cell monolayers and treated with 0.2 ml 10% trichloroacetic acid. Cell monolayers were washed with an additional 0.1 ml PBS and the wash was pooled with the initial reaction medium. The protein precipitate was removed by centrifugation at 8500 *g* for 5 min. Supernatants were treated with 70 μl of 6 N NaOH, and applied to a 1 ml Dowex-1 (Sigma Chemical, St. Louis, MO) column. The ^3H_2O, which is an end product of oxidation, passes through the column. This sample, together with a 1-ml water wash, was directly quantitated by scintillation counting in 10 ml EcoLite (ICN, Irvine, CA).

To determine total cellular protein of cultures used for oxidation assays, 1 ml of water was added to cell monolayers after removal of reaction medium and cells were subjected to 3 cycles of freezing (−70°C) and thawing (37°C). Proteins were determined using a modified Bradford protein assay reagent (Bio-Rad, Hercules, CA).

Statistical analyses

Values for 2DE protein levels, hepatic lipase activities (9), and fatty acid oxidation rates are given as mean ± SD. The Student's *t*-test was used to test for differences between *fld* and wild-type mice. Differences were considered statistically significant at $P < 0.05$.

RESULTS

Accumulation of triglyceride in hepatocytes from neonatal *fld* mice

As originally described, *fld*/*fld* mice (referred to henceforth as *fld*) can be distinguished from their unaffected littermates in the first few postnatal days by smaller body size, the appearance of a swollen abdomen due to hepatomegaly, and the distinctive pale fatty liver (3). Examination of liver morphology by light microscopy revealed microvesicular steatosis in parenchymal cells from neonatal *fld* mice (**Fig. 1b**), compared to the small sparse lipid droplets in the liver of wild-type littermates (Fig. 1a). Triglyceride concentration in neonatal *fld* mice was elevated 6-fold compared to wild-type mice (43.7 vs. 7.6 μg triglyceride/mg liver protein). In addition, the *fld* hepatocytes were hypertrophic due to the large mass of intracellular triglyceride, resulting in the characteristic hepatomegaly observed in neonatal *fld* mice. In contrast to *fld* neonates, parenchymal cells of adult *fld* mice (Fig. 1d) appear similar to those from their wild-type counterparts (Fig. 1c) with a normal number and distribution of lipid droplets.

At the ultrastructural level, liver parenchymal cells from *fld* neonates exhibit only subtle differences compared to those from wild-type mice (see **Fig. 2**). Mitochondria and peroxisomes are evident in both wild-type and *fld* cells, and often occur in direct physical contact with lipid droplets. In some *fld* cells, we detected unusual cytoplasmic structures that appear to consist of membrane stacks or whorls (arrows in Fig. 2c), the origin of which is unknown. Analysis by electron microscopy revealed no differences in liver morphology in mature *fld* mice (not shown).

Altered expression levels of peroxisome proliferator-regulated proteins in *fld* fatty liver

The initial characterization of the *fld* fatty liver revealed altered hepatic expression levels of three proteins involved in lipid metabolism, hepatic lipase, apolipoprotein A-IV, and apolipoprotein C-II (3). To produce a comprehensive overview of protein expression patterns in the *fld* fatty liver, we performed quantitative 2DE of liver proteins from *fld* and wild-type mice at 5 days of age. Equivalent amounts of protein from liver homogenates were subjected to isoelectric focusing followed by SDS polyacrylamide gel electrophoresis, and the resulting protein patterns were analyzed for qualitative and quantitative differences (8). Liver samples from each of 10 wild-type and 10 *fld* mice were examined. A typical 2DE pattern of hepatic proteins from an *fld* fatty liver is shown in **Fig. 3**. While 2DE patterns resulting from *fld* and wild-type livers were qualitatively similar, quantitation of more than 400 distinct proteins detected by Coomassie Blue staining revealed significantly altered levels ($P < 0.001$) of 24 proteins in the fatty liver compared to wild-type liver (arrows in Fig. 3 and **Table 1**). Of these, 22 proteins were expressed at significantly higher levels in the fatty liver, whereas only 2 proteins (spots 36 and 112) were diminished in the *fld* mice (Table 1). In contrast to the pronounced difference in protein expression pattern be-

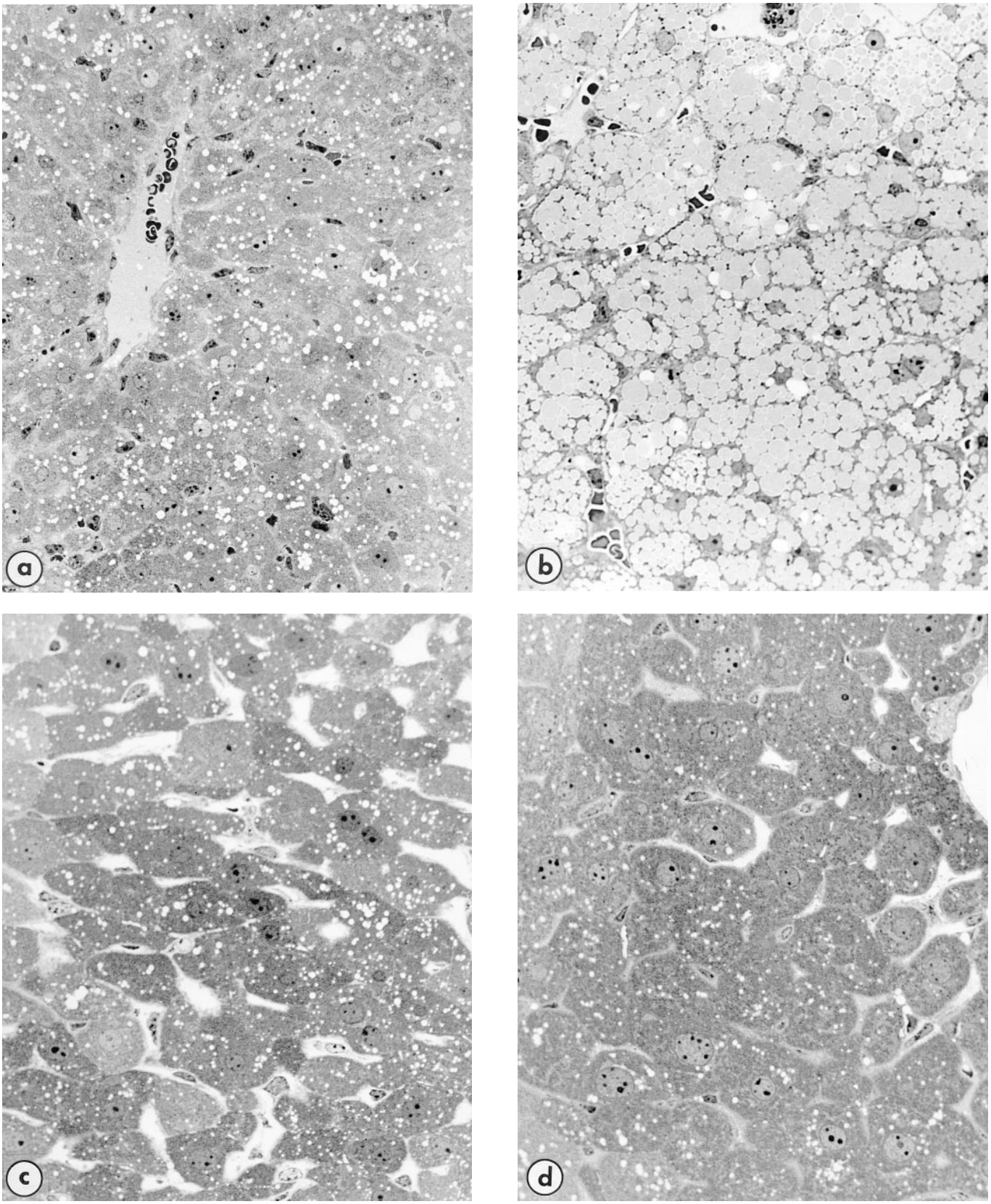

Fig. 1. Light micrographs of liver sections from 9-day and 3-month-old *fld/fld* and wild-type mice. Liver sections were prepared from wild-type and *fld/fld* mice, stained with toluidine blue, and viewed at a magnification of 495×. (a) Hepatocytes from 9-day-old wild-type mice contain small, sparse lipid droplets, visible as clear spherical structures (lipid droplets are dissolved with alcoholic sodium hydroxide during tissue preparation). (b) Hepatocytes from 9-day-old *fld/fld* mice are hypertrophic and characterized by extensive accumulation of large lipid droplets. At 3 months of age, hepatocytes from wild-type (c) and *fld/fld* mice (d) appear similar, with only sparse lipid droplets and no hypertrophy.

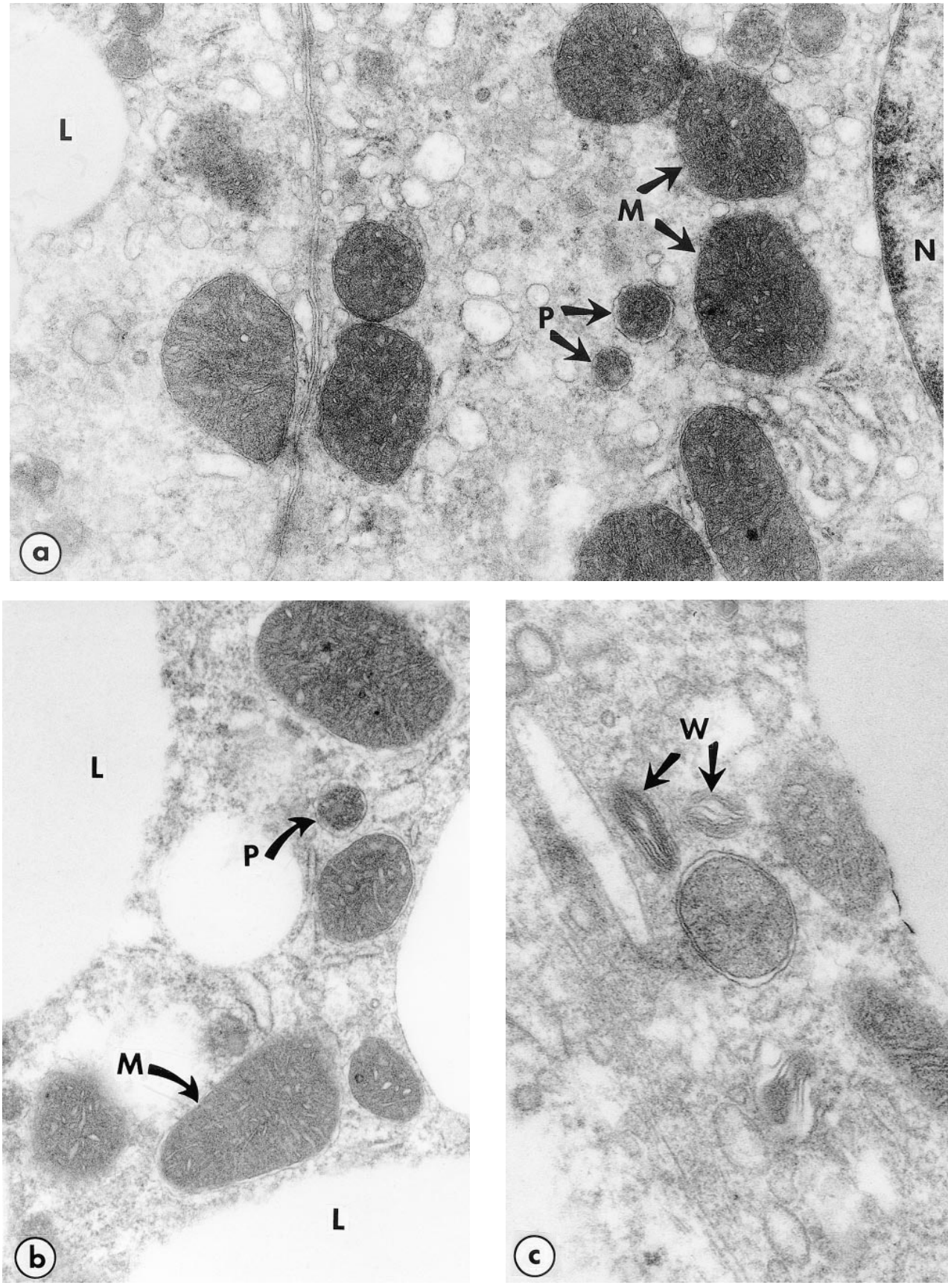

Fig. 2. Electron micrographs of hepatocytes from 9-day-old *fld/fld* and wild-type mice. Thin sections of liver were prepared, stained with lead and uranium salts, and viewed at a magnification of 30,000× (panels a and b) or 60,000× (panel c). (a) In the wild-type liver, note adjacent hepatocytes showing normal ultrastructural appearance. N, nucleus; L, lipid droplet; M, mitochondria; P, peroxisome. (b) Hepatocytes from *fld/fld* exhibit larger, abundant lipid droplets. (c) *fld/fld* hepatocyte with whorls or membrane stacks (W).

Fig. 3. Representative 2-dimensional gel electrophoresis pattern from livers of 5-day-old *fld/fld* mice. Proteins with altered abundance in *fld/fld* compared to wild-type liver samples are indicated by arrows and protein spot numbers that have been assigned in the Argonne National Laboratory Mouse 2DE Database (8, 13). The gel is oriented with acidic proteins to the left, basic proteins to the right, high molecular weight proteins toward the top, and low molecular weight proteins toward the bottom, with molecular mass standards indicated along the left edge ($\times 10^{-3}$ kDa). All proteins indicated with arrows exhibited elevated levels in *fld/fld* compared to wild-type mice, except spots 36 and 112, which were diminished in *fld/fld* liver. The relative levels of the indicated proteins in wild-type and *fld* liver are presented in Table 1. (Note that spot number 98 in the figure was subsequently determined not to exhibit altered levels in *fld* vs. wild-type and is not included in Table 1.)

tween *fld* and wild-type at 5 days of age, there are few apparent differences in expression levels between adult *fld* and wild-type liver, indicating that protein expression levels in *fld* liver are largely normalized after the fatty liver is resolved (data not shown).

A comparison of the 2DE patterns with the mouse protein database maintained at Argonne National Laboratory (8, 13) allowed identification of some of the 24 proteins with altered expression in the fatty liver of 5-day-old *fld* mice. Proteins with elevated expression levels in the fatty liver include keratin (spot 23), β-actin (spot 29), and γ-actin (spot 185). Additionally, spot 245 was identified as apoA-IV by immunoblot analysis using specific antibodies (data not shown). ApoA-IV protein levels are elevated 7-fold in the *fld* fatty liver (Table 1), reflecting the previously described elevation in apoA-IV mRNA (3). Expression levels of a related protein, apoA-I (spot 294 in the mouse protein database), are not altered in the fatty liver.

Additional information in the 2DE database revealed that a majority of the 24 proteins with altered expression in *fld* fatty liver respond to peroxisome proliferating agents. These chemicals induce a variety of responses in liver: increased peroxisome number, hypertrophy, hepatocarcinogenesis, and altered expression levels of specific proteins in peroxisomes, mitochondria, microsomes, and cytoplasm (14–17). These compounds are also effective in lowering serum triglyceride levels, an effect which has been attributed to increased expression levels of several fatty acid oxidation genes, including enzymes for fatty acid β-oxidation in peroxisomes and mitochondria, and ω-oxidation in microsomes. For 17 of the 24 proteins with altered expression levels in *fld* fatty liver, information is available concerning response to four different peroxisome proliferating compounds (clofibrate, cipofibrate, di-(2-ethylhexyl)-phthalate, and [4-chloro-6(2,3-xylidino)2-pyrimidinylthio]acetic acid, known as WY-14,463) (8). Of these 17 proteins, 88% (15/17) respond to one or more peroxisome proliferating agents, and the majority (65%; 11/17) respond to one specific proliferating chemical, WY-14,463. This represents twice the frequency of all data-

TABLE 1.

Spot Number	Molecular Weight	Protein Level		fld/wt	Peroxisome Prolif. Response
		Wild-type	*fld*		
1	72,500	66,133 (17.7%)	105,991 (14.4%)	1.60	+
23	48,000	17,963 (11.3%)	28,204 (18.9%)	1.57	+
29	43,200	18,024 (16.3%)	38,106 (15.1%)	2.11	+
36	35,700	40,683 (12.2%)	14,969 (28.2%)	0.37	+
112	33,500	5221 (17.5%)	2438 (34.8%)	0.47	+
181	47,300	2368 (11.9%)	3388 (17.6%)	1.43	+
185	44,700	4069 (33.6%)	9006 (30.3%)	2.21	+
198	62,000	3822 (13.0%)	6416 (9.0%)	1.68	+
206	34,000	5036 (13.7%)	13,318 (22.7%)	2.64	+
223	62,500	1504 (12.8%)	2305 (10.5%)	1.53	+
227	25,800	2147 (54.0%)	4571 (23.2%)	2.13	+
245	43,000	7306 (34.3%)	53,163 (20.4%)	7.28	−
258	61,700	2262 (6.8%)	3163 (8.7%)	1.40	+
301	38,700	2286 (11.6%)	3149 (11.6%)	1.38	+
316	27,900	2944 (10.4%)	7154 (16.2%)	2.43	+
395	33,400	1612 (29.1%)	3252 (14.9%)	2.02	−
421	49,500	957 (11.2%)	1311 (12.9%)	1.37	n.d.
433	60,600	1849 (12.0%)	3162 (12.2%)	1.71	n.d.
436	34,000	2007 (18.9%)	4384 (30.4%)	2.18	+
485	43,500	1617 (18.3%)	2339 (15.3%)	1.45	n.d.
1038	49,000	1042 (27.3%)	1853 (17.0%)	1.78	n.d.
1061	54,000	947 (32.2%)	1904 (27.7%)	2.01	n.d.
1067	43,400	1611 (33.4%)	3799 (21.9%)	2.36	n.d.
1096	58,000	1427 (47.3%)	2898 (17.2%)	2.03	n.d.

Liver protein homogenates from 5-day-old wild-type and *fld* mice were analyzed by quantitative 2DE as described in Methods. The 24 proteins listed were present at significantly different levels in the livers of *fld/fld* compared to wild-type (+/?) mice ($P < 0.001$). Spot numbers correspond to proteins in the 2DE database (8, 13). Molecular weights were estimated from migration position compared to standards. Relative protein levels in wild-type and *fld* samples were determined from integrated spot densities and are given in arbitrary units with the coefficient of variation for samples from 10 animals of each phenotype (shown in parentheses). The fld/wt value represents the ratio of *fld* to wild-type protein levels. Proteins known to be altered in abundance by treatment with peroxisome proliferating chemicals are denoted by "+"; proteins that do not respond are denoted "−"; and proteins for which response to peroxisome proliferators has not been determined by are denoted n.d.

base proteins that have been tested for response to WY-14,463 (94/287) (8).

Reduced efficiency of fatty acid oxidation in *fld* hepatocytes

As peroxisome proliferators are known to induce mitochondrial and peroxisomal proteins that function in fatty acid β-oxidation, we measured fatty acid oxidation rates in hepatocytes isolated from *fld* and wild-type mice. We first determined that hepatocytes isolated from 12-day-old *fld* mice can be grown in culture for up to 4 days and maintain the hallmark features of the fatty liver, including the characteristic lipid accumulation (data not shown), a 2-fold reduction in hepatic lipase activity (0.85 ± 0.17 mU/ml culture medium for *fld* compared to 1.48 ± 0.10 mU/ml for wild-type), and elevated apoA-IV mRNA levels. As shown in **Fig. 4**, mRNA levels for apoA-I are similar between wild-type and *fld* hepatocytes (lower arrow), while apoA-IV mRNA levels are dramatically increased in the *fld* hepatocytes (upper arrow). The preservation of these features of the *fld* fatty liver in isolated hepatocytes indicates that they result from an intrinsic aberration in metabolism at the cellular level, and indicate that the isolated cells are a valuable model in which to study the biochemical basis for development of the fatty liver.

For fatty acid oxidation studies, hepatocytes from *fld* and wild-type mice were isolated by collagenase perfusion, cultured overnight, and then incubated with a radiolabeled fatty acid substrate ([9,10(n)-^{3}H]-palmitate) for 2 h. The release of ^3H_2O was quantitated as a measure of the

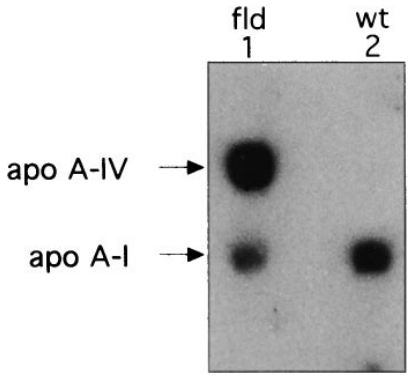

Fig. 4. mRNA levels for apoA-IV and apoA-I in cultured hepatocytes prepared from 12-day-old *fld/fld* and wild-type mice. Isolated hepatocytes from 12-day-old *fld/fld* and wild-type (wt) mice were maintained in culture for 4 days and the total RNA was isolated. Northern blot analysis was performed with 10 μg of RNA. Hepatocytes from *fld/fld* mice (lane 1) exhibit approximately 90-fold higher levels of mRNA for apoA-IV (upper band) than cells from wild-type littermates (lane 2), although mRNA levels for apoA-I (lower band) are similar in both.

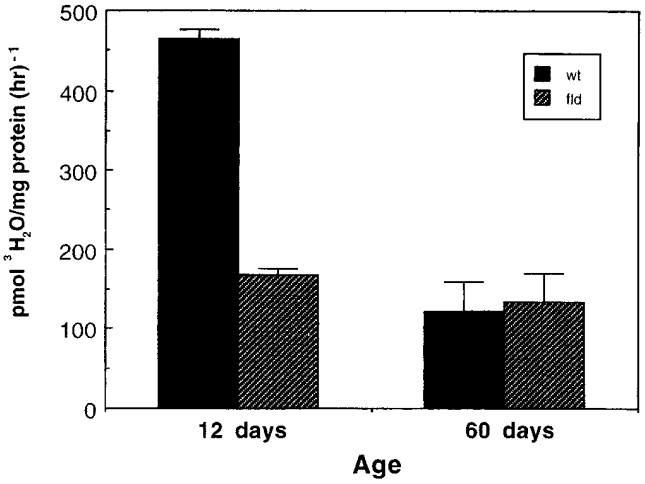

Fig. 5. Palmitate oxidation in hepatocytes isolated from *fld/fld* and wild-type mice at 12 and 60 days of age. Hepatocytes were isolated by collagenase perfusion and grown in culture overnight. Cells were incubated with [^{3}H]palmitate, and the formation of ^3H_2O was quantitated as a measure of the rate of palmitate oxidation (see Methods). Palmitate oxidation rates for individual samples were normalized on the basis of total cellular protein. Each bar value represents the mean of 6–8 experimental points derived from two or more independent assays. Error bars indicate SD.

rate of β-oxidation (12). We chose palmitate for this assay because it can serve as a substrate for oxidation in both peroxisomes and mitochondria, and therefore would measure overall β-oxidation efficiency in the *fld* hepatocytes.

Results of the palmitate oxidation assay are shown in **Fig. 5**. In assays performed with hepatocytes from 12-day-old mice, *fld* cells exhibited a 60% reduction in the rate of palmitate oxidation compared to cells from wild-type mice. In contrast, oxidation efficiency in hepatocytes from adult *fld* mice (60 days of age) that no longer accumulate intracellular triglyceride was similar to that of age-matched wild-type mice (Fig. 5). Thus, the rate of palmitate oxidation is diminished in neonatal but not adult *fld* hepatocytes. These results are consistent with a role for reduced fatty acid oxidation contributing to the accumulation of triglyceride in the liver of neonatal *fld* mice, or as a secondary phenotype arising from the triglyceride accumulation.

DISCUSSION

We present here a further characterization of the altered protein expression and lipid metabolism in the fatty liver of the *fld* mutant mouse. It is clear from examination of both liver sections and isolated hepatocytes that the accumulation of lipid in the liver of neonatal *fld/fld* mice occurs within the parenchymal cells and cannot be attributed to other cell types such as Kupffer cells or fat-storing Ito cells. We also determined that isolated neonatal hepatocytes grown in culture up to 4 days continue to exhibit characteristic features of the fatty liver phenotype, including cytoplasmic lipid droplets, elevated apoA-IV mRNA levels, and reduced hepatic lipase activity. This retention of the mutant phenotype in cultured *fld* hepatocytes suggests that the fatty liver develops as a result of an intrinsic defect and is not caused by the hypertriglyceridemia that also persists during the neonatal period.

An overview of hepatic protein expression patterns associated with microvesicular steatosis has not, to our knowledge, been previously reported. We have utilized quantitative 2DE to compare protein expression patterns in the fatty liver of neonatal *fld* mice with that of their wild-type counterparts, and detected 24 proteins with altered expression levels. Fifteen of the proteins that exhibit increased expression levels in the *fld* liver are known to be altered in abundance by peroxisome proliferating compounds (Table 1 and ref. 8). Although the *fld* mutation and peroxisome proliferator compounds both elicit altered expression levels of several of the same proteins, notable differences between the two conditions are apparent. Our morphological studies revealed that the *fld* fatty liver does not exhibit pronounced peroxisome proliferation or increased fatty acid oxidation, suggesting that the proteins induced in the *fld* liver represent a subset of peroxisome proliferator-regulated proteins from cellular compartments other than peroxisomes. Another notable difference is that peroxisome proliferators decrease the expression levels of apoA-IV (18), in contrast to the dramatically elevated apoA-IV levels observed in the *fld* liver. Although the function of apoA-IV is not well understood, it has been proposed that this protein has a role in intracellular triglyceride storage or synthesis of triglyceride-rich lipoproteins (19), and its elevated expression in the fatty liver may therefore represent a secondary response to the accumulated lipid.

Our studies of morphology and protein expression in the *fld* fatty liver are consistent with a scenario in which triglyceride accumulates in the liver as a result of the *fld* gene mutation, triggering a secondary response in which a subset of peroxisome proliferator-activated proteins are induced by the accumulated lipid. Although the identity and function of most of the induced proteins is not yet known, an attractive hypothesis is that they may have a role in the subsequent mobilization or metabolism of triglyceride from the liver which occurs as the *fld* mice mature. The resolution of the fatty liver at 13–18 days of age coincides temporally with the developmental induction of both increased capacity for fatty acid oxidation and efficient secretion of triglycerides in the form of very low density lipoprotein. Specifically, levels of the acyl-CoA dehydrogenases, which catalyze the first step of mitochondrial fatty acid oxidation, are low at birth and then increase several-fold to peak at postnatal days 10–14, at a time when the *fld* fatty liver begins to resolve (20). Similarly, the capacity for hepatic secretion of triglyceride-rich very low density lipoprotein is limited in neonatal rats, but increases to near adult levels shortly before the age of weaning (typically 18–21 days) (21). Clearly, it is of interest to determine whether proteins involved in these processes are among those that exhibit altered expression levels in the fatty liver; we are currently approaching this problem by isolating differentially expressed mRNA species from

the fatty liver and determining the cDNA sequence to identify the corresponding protein products.

The *fld* gene has not yet been identified, but has been mapped to proximal chromosome 12 in the mouse, a region which corresponds to the short arm of human chromosome 2 (6). The chromosomal localization of the mutant gene makes it possible to exclude previously mapped genes encoding lipid metabolism proteins, peroxisome proliferator activated receptors, and known neurological mutations (3–5, 22–24). There are no obvious candidate genes which localize to the appropriate genomic region, suggesting that the *fld* locus may represent a novel gene; efforts are underway to identify this gene by a positional cloning strategy. These studies are likely to provide new insights into the metabolic basis for the development of fatty liver and lipid homeostasis in the newborn.

We thank Krista Mishler (participant in the Argonne National Laboratory Division of Educational Programs SERS program) for performing 2-dimensional gel electrophoresis experiments. These studies were supported by grants from the National Institutes of Health (HL 28481, K. Reue and M. H. Doolittle), American Heart Association (Established Investigator Awards to M. H. Doolittle and K. Reue), and The U.S. Department of Energy, Office of Biological and Environmental Research (Contract W-31-109-ENG-38 to C. S. Giometti). S. Rehnmark was supported by the Swedish Natural Science Research Council.

Manuscript received 9 January 1998 and in revised form 15 June 1998.

REFERENCES

1. Day, C. P. and Yeaman, S. J. 1994. The biochemistry of alcohol-induced fatty liver. *Biochim. Biophys. Acta.* **1215:** 33–48.
2. Day, C. P., O. F. W. James, A. S. J. M. Brown, M. K. Bennett, I. N. Fleming, and S. J. Yeaman. 1993. The activity of the metabolic form of hepatic phosphatidate phosphohydrolase correlates with the severity of alcoholic fatty liver in human beings. *Hepatology.* **18:** 832–838.
3. Langner, C. A., E. H. Birkenmeier, O. Ben-Zeev, M. C. Schotz, H. O. Sweet, M. T. Davisson, and J. I. Gordon. 1989. The fatty liver dystrophy (*fld*) mutation. A new mutant mouse with a developmental abnormality in triglyceride metabolism and associated tissue-specific defects in lipoprotein lipase and hepatic lipase activities. *J. Biol. Chem.* **264:** 7994–8003.
4. Reue, K. and M. H. Doolittle. 1996. Naturally occurring mutations in mice affecting lipid transport and metabolism. *J. Lipid Res.* **37:** 1387–1405.
5. Langner, C. A., E. H. Birkenmeier, K. A. Roth, R. T. Bronson, and J. I. Gordon. 1991. Characterization of the peripheral neuropathy in neonatal and adult mice that are homozygous for the fatty liver dystrophy (*fld*) mutation. *J. Biol. Chem.* **266:** 11955–11964.
6. Rowe, L. B., H. O. Sweet, J. I. Gordon, and E. H. Birkenmeier. 1996. The *fld* mutation maps near to but distinct from the *Apob* locus on mouse Chromosome 12. *Mamm. Genome.* **7:** 555–557.
7. Carr, T. P., C. J. Andresen, and L. L. Rudel. 1993. Enzymatic determination of triglyceride, free cholesterol, and total cholesterol in tissue lipid extracts. *Clin. Biochem.* **26:** 39–42.
8. Giometti, C. S., J. Taylor, and S. L. Tollaksen. 1992. Mouse liver protein database: a catalog of proteins detected by two-dimensional gel electrophoresis. *Electrophoresis.* **13:** 970–991.
9. Doolittle, M. H., H. Wong, R. C. Davis, and M. C. Schotz. 1987. Synthesis of hepatic lipase in liver and extrahepatic tissues. *J. Lipid Res.* **28:** 1326–1333.
10. Nilsson-Ehle, P. and M. C. Schotz. 1976. A stable, radioactive substrate emulsion for assay of lipoprotein lipase. *J. Lipid Res.* **17:** 536–541.
11. Reue, K., D. A. Purcell-Huynh, T. H. Leete, M. H. Doolittle, A. Durstenfeld, and A. J. Lusis. 1993. Genetic variation in mouse apolipoprotein A-IV expression is determined pre- and post-transcriptionally. *J. Lipid Res.* **34:** 893–903.
12. Moon, A. and W. J. Rhead. 1987. Complementation analysis of fatty acid oxidation disorders. *J. Clin. Invest.* **79:** 59–64.
13. Argonne National Laboratory Mouse Liver 2DE Protein Database. http://www.anl.gov/CMG/PMG/projects/index_mouse.html.
14. Auwerx, J. 1992. Regulation of gene expression by fatty acids and fibric acid derivatives: an integrative role for peroxisome proliferator activated receptors. The Belgian Endocrine Society Lecture 1992. *Horm. Res.* **38:** 269–277.
15. Reddy, J. K. and G. P. Mannaerts. 1994. Peroxisomal lipid metabolism. *Annu. Rev. Nutr.* **14:** 343–370.
16. Schoonjans, K., B. Staels, and J. Auwerx. 1996. Role of the peroxisome proliferator-activated receptor (PPAR) in mediating the effects of fibrates and fatty acids on gene expression. *J. Lipid Res.* **37:** 907–925.
17. Motojima, K. 1993. Peroxisome proliferator-activated receptor (PPAR): structure, mechanisms of activation and diverse functions. *Cell Struct. Funct.* **18:** 267–277.
18. Staels, B., A. von Tol, T. Andreu, and J. Auwerx. 1992. Fibrates influence the expression of genes involved in lipoprotein metabolism in a tissue-selective manner. *Arteriosclerosis.* **12:** 286–294.
19. LeBoeuf, R. C., M. Caldwell, and E. Kirk. 1994. Regulation by nutritional status of lipids and apolipoproteins A-I, A-II, and A-IV in inbred mice. *J. Lipid Res.* **35:** 121–133.
20. Nagao, M., B. Parimoo, and K. Tanaka. 1993. Developmental, nutritional, and hormonal regulation of tissue-specific expression of the genes encoding various acyl-CoA dehydrogenases and alpha-subunit of electron transfer flavoprotein in rat. *J. Biol. Chem.* **268:** 24114–24124.
21. Frost, S. C., W. A. Clark, and M. A. Wells. 1983. Studies on fat digestion, absorption, and transport in the suckling rat IV: in vivo rates of triacylglycerol secretion by intestine and liver. *J. Lipid Res.* **24:** 899–903.
22. Reue, K., Y-R. Xia, V. W. Shi, R. D. Cohen, C. Welch, and A. J. Lusis. 1996. Localization of mouse peroxisome proliferator-activated receptor γ on Chromosome 6. *Mamm. Genome.* **7:** 390–391.
23. Cohen, R. D., C. Welch, Y-R. Xia, A. J. Lusis, and K. Reue. 1996. Localization of mouse peroxisome proliferator-activated receptor δ (*Ppard*) on Chromosome 17 near colipase (*Clps*). *Mamm. Genome.* **7:** 557–558.
24. Reue, K., and R. D. Cohen. 1996. *Acads* gene deletion in BALB/cByJ mouse strain occurred after 1981 and is not present in BALB/cByJ-*fld* mutant mice. *Mamm. Genome.* **7:** 694–695.